

See discussions, stats, and author profiles for this publication at: <https://www.researchgate.net/publication/317433310>

Atomic mapping of structural distortions in 109° domain patterned BiFeO₃ thin films

Article in Journal of Materials Research · June 2017

DOI: 10.1557/jmr.2017.206

CITATIONS

0

READS

12

6 authors, including:



[W.Y. Wang](#)

Chinese Academy of Sciences

5 PUBLICATIONS 7 CITATIONS

[SEE PROFILE](#)



[Y.L. Zhu](#)

Institute of Metal Research, Chinese Academ...

84 PUBLICATIONS 516 CITATIONS

[SEE PROFILE](#)



[Yunlong Tang](#)

Chinese Academy of Sciences

19 PUBLICATIONS 62 CITATIONS

[SEE PROFILE](#)



[Meng Jiao Han](#)

Chinese Academy of Sciences

1 PUBLICATION 0 CITATIONS

[SEE PROFILE](#)

Some of the authors of this publication are also working on these related projects:



functional oxide films [View project](#)



Atomic Level 1D Structural Modulations at the Negatively Charged Domain Walls in BiFeO₃ Films [View project](#)

All content following this page was uploaded by [W.Y. Wang](#) on 20 June 2017.

The user has requested enhancement of the downloaded file. All in-text references [underlined in blue](#) are added to the original document and are linked to publications on ResearchGate, letting you access and read them immediately.

ARTICLES

Atomic mapping of structural distortions in 109° domain patterned BiFeO₃ thin films

Wen-Yuan Wang

Shenyang National Laboratory for Materials Science, Institute of Metal Research, Chinese Academy of Sciences, Shenyang 110016, China; and Science and Technology on Surface Physics and Chemistry Laboratory, 621908 Jiangyou, Sichuan, China

Yin-Lian Zhu, Yun-Long Tang, Meng-Jiao Han, and Yu-Jia Wang

Shenyang National Laboratory for Materials Science, Institute of Metal Research, Chinese Academy of Sciences, Shenyang 110016, China

Xiu-Liang Ma^{a)}

Shenyang National Laboratory for Materials Science, Institute of Metal Research, Chinese Academy of Sciences, Shenyang 110016, China; and School of Materials Science and Engineering, Lanzhou University of Technology, 730050 Lanzhou, China

(Received 18 January 2017; accepted 8 May 2017)

Structural distortions at the nanoscale are delicately linked with many exotic properties for ferroic thin films. Based on advanced aberration corrected scanning transmission electron microscopy, we observe BiFeO₃ thin films with variant tensile strain states and demonstrate at an atomic scale the interplay of intrinsic spontaneous structural distortions with external constraints. Structural parameters (the rhombohedral distortion and domain wall shear distortion) under zero (BiFeO₃/GdScO₃) and 1.5% (BiFeO₃/PrScO₃) lateral strain states are quantitatively analyzed which are suppressed within a few unit cells near the film/substrate interfaces. In particular, an interfacial layer with asymmetrical lattice distortions (enhanced and reduced out-of-plane lattice spacing) on the two sides of 109° domain wall is resolved. These structural distortions near the film/substrate interface in ferroic thin films reveal intense tanglement of intrinsic distortions of BiFeO₃ with external boundary conditions, which could provide new insights for the development of nanoscale ferroelectric devices.

I. INTRODUCTION

Due to the interplay between order parameters and external stimulations, ferroics such as ferroelectrics, ferromagnetics, and multiferroics offer many advantages in the field of information storage, sensors and, actuators.^{1–3} The strain related structural distortion, which often connects to the order parameters of ferroics, has been demonstrated to be an effective degree of freedom to manipulate the properties of ferroic materials.^{4,5} The enhancement of ferroelectricity, triggering ferroelectricity, and multiferroelectricity can be achieved in thin films where structural distortions are naturally imbedded through substrate constraints.^{6–8} In addition, the spontaneous structural distortion, an intrinsic feature of ferroic materials below Curie temperature, interacts with the substrate constraint so that novel strains states⁹ and domain structures¹⁰ can emerge. Understanding such kind of interaction, especially how the lattice distortions at an atomic scale behave, would be of crucial to underline the relevant physical natures as well as

to potentially manipulate the related physical properties for nanoscale ferroic devices.

BiFeO₃, one of the most widely studied ferroics, can show rich phase states,^{11–13} controllable ferroelectric variants,^{14,15} and versatile domain wall configurations¹⁶ in terms of heterofilms. Tetragonal BiFeO₃ with a giant *c/a* ratio can be stabilized if compressive strain is larger than –4.5%,¹² while the orthogonal phase is predicted to exist when tensile strain is over 1%.¹³ A stripe-like domain pattern or irregular domain pattern can be produced by using appropriate substrates.¹⁴ For BiFeO₃, the effect of heterostructures, in fact, also reflects on mediating the coherent structural distortions that include the rhombohedral distortion and domain wall shear distortion. Theoretical studies based on elastic theory have been done to dealing with the effect of substrate constraints on the rhombohedral distortion.^{17–20} Experimentally, studies based on reciprocal methods or real space methods have been carried out and mainly focused on domain pattern geometries.^{14,15,21} For example, Chu et al. showed that in-plane lattice constraints of an orthoscorandate substrate allow two kinds of rhombohedral distortions (ferroelectric variants) existing in films based on piezoelectric force microscopy (PFM) analysis,¹⁵ while Giencke et al. reported that by using three dimensional constraints of substrates, only one kind of

Contributing Editor: Cewen Nan

^{a)}Address all correspondence to this author.

e-mail: xlma@imr.ac.cn

DOI: 10.1557/jmr.2017.206

rhombohedral distortion can be achieved.²¹ Although advanced aberration corrected transmission electron microscope has been applied to study the atomic structures of BiFeO₃ thin films.^{22–25} A direct mapping on an atomic scale of the interaction between substrate constraints and the coherent structural distortions in related ferroics, especially for BiFeO₃, is inadequate up to now.

Here, by means of advanced aberration corrected transmission electron microscope, we studied on atomic scale the interplay of substrate constraints and the coherent structural distortions in 109° domain patterned BiFeO₃ thin films. Structural parameters including the rhombohedral distortion and domain wall shear distortion near the interface are quantitatively demonstrated. An interfacial layer with asymmetric distributed lattice distortions emerges. The result implies that, by making use of certain internal structural distortions and boundary conditions, additional structural features could be triggered at the local area near/at heterointerfaces in BiFeO₃ thin films, which could be helpful for exploring novel properties for related nanoscale ferroelectric devices.

II. EXPERIMENT

(001)_P oriented BiFeO₃ thin films were epitaxially grown on (110)_O oriented GdScO₃ and PrScO₃ single crystal substrates by pulsed laser deposition (PLD) (where the P and O subscripts stand for pseudocubic and orthorhombic index, respectively). The pseudocubic lattice constants of GdScO₃ and PrScO₃ are about 3.97 Å and 4.02 Å,²⁶ indicating almost zero lateral misfit strain for BiFeO₃/GdScO₃, whereas a tensile strain as high as 1.5% for BiFeO₃/PrScO₃. The growth temperature was 680 °C, with an oxygen pressure of 13 Pa and a laser frequency of 10 Hz. After deposition, the films were *in situ* annealed in pure O₂ under 5 × 10⁴ Pa for 30 min before cooled down to room temperature. Scanning transmission electron microscopy (STEM) samples were prepared by conventional methods including slicing, gluing, grinding, and final ion milling. A Titan G² 60–300 microscope (FEI Company, Eindhoven, The Netherlands) with a high-brightness field-emission gun and double aberration (Cs) correctors was used to acquire STEM images. A quantitative analysis of the atomic-resolution STEM images was based on the plug-in in Matlab which determines the positions of atoms by fitting the intensity profiles using two-dimensional Gaussian fittings.²⁷ The substrates are used as references to correct possible drift distortions.

III. RESULTS

A. General information

The bulk BiFeO₃ has a distorted perovskite structure (space group *R*3c) with pseudo-cubic unit cell of $a =$

3.965 Å and $\alpha = 89.4^\circ$, as shown in Fig. 1(a). The spontaneous polarization (Ps) of BiFeO₃ is along $\langle 111 \rangle_P$ directions, thus eight ferroelectric variants and four ferroelastic variants can exist. The corresponding ferroelectric domain configurations are 109°, 71° and 180°, respectively. In the present work, we focused on the 109° domain pattern since it can be easily obtained^{15,28} and many novel properties were found on such domain walls.^{29,30} To describe the structural features of BiFeO₃ in an appropriate way, we introduce lattice spacing (L_x , L_y) and lattice rotation (R_x , R_y) as structural variables in Fig. 1(b). The intrinsic structural nature of the 109° domain pattern and influence of substrate constraints then can be studied in detail. (001)_P oriented BiFeO₃ thin films were grown on (110)_O GdScO₃ and (110)_O PrScO₃ single crystal substrates using PLD. The (110)_O oriented scandate substrate has a monoclinic distorted constraint onto BiFeO₃ which can result in a 109° domain pattern.^{25,31} Figures 1(c) and 1(d) show the domain geometries of two systems, BiFeO₃ (~60 nm)/GdScO₃ and BiFeO₃ (~50 nm)/PrScO₃, respectively. The stripe-like domain geometry with periodic bright and dark contrast in Figs. 1(c) and 1(d) convinces the existence of the 109° domain pattern.^{25,32,33} The BiFeO₃/GdScO₃ thin film system with negligible lattice mismatch, providing minimized external constraints, can serve as a reference to study the structural feature of the 109° domains, while the

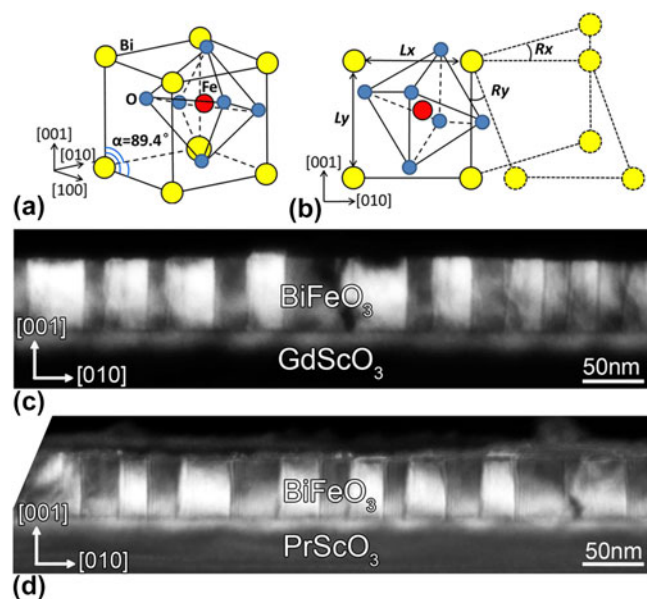


FIG. 1. (a) A schematic model of the pseudocubic unit cell of BiFeO₃. Note that the interangle of three $\langle 100 \rangle_P$ axes is 89.4° representing the spontaneous rhombohedral distortion (the P subscript stands for pseudocubic index). (b) Structural variations of BiFeO₃. L_x and L_y represent the local lattice spacing while R_x and R_y represent the local lattice rotation. (c–d) Dark field images of cross-sectional BiFeO₃/GdScO₃ and BiFeO₃/PrScO₃ thin films, respectively.

BiFeO₃/PrScO₃ thin film system with a lattice mismatch as large as 1.5% can offer an intense substrate constraint onto 109° domains.

B. Structural features of unstrained 109° domains

The 109° domains of BiFeO₃ are both ferroelectric and ferroelastic, which means that the adjacent domains have different distortion directions, as shown in Fig. 2(a). Each ferroelectric variant obtains a mismatch angle δ with the substrate, thus the adjacent domains have a mismatch angle of 2δ . This mismatch angle stands for a kind of spontaneous structural distortion (rhombohedral distortion). In fact, the structure of the 109° domain pattern far away from the film/substrate interface for BiFeO₃ grown on GdScO₃ could resemble the ideal situation of the relaxed 109° domain in Fig. 2(a) because the influences of the misfit strain and interface are minimized in such a system. Figure 2(b) is an atomic-resolution high angle annular dark field scanning transmission electron microscopy (HAADF-STEM) image revealing a 109° domain pattern far away from the BiFeO₃/GdScO₃ interface. As the intensity of the HAADF-STEM image connects to the atomic number (roughly proportional to Z^2),^{10,23,24} element species can be deduced according to the intensity of atomic columns. Therefore, in Fig. 2(b), the big bright spots are Bi columns and small weak spots are Fe columns. For the O columns, they are invisible in the HAADF mode due to its weak scattering abilities on electrons. It is also noticeable that the relative displacement of Fe sublattice in each unit cell can be clearly resolved which is inverse with the Ps direction [colored arrow in Fig. 2(b)].^{10,23,24} The rhombohedral distortion visualized by the mismatch angle 2δ of nearby domains can be noticed according to the relative rotation of the horizontal lattice (Bi sublattice) of nearby domains, as shown in Fig. 2(b). The location of the domain wall can be determined based on the directions of sublattice displacements, and the obvious lattice shear distortion can be noticed at the domain wall [marked by the two white arrows and the superposed structural model inserted in Fig. 2(b)]. Note that such a domain wall distortion is concentrated on only one unit cell in width which has been also reported by several studies previously.^{24,34,35} The above structural features of 109° domains in Fig. 2(b) are further demonstrated in Figs. 2(c) and 2(d) in a quantitative way, where line profiles of L_x , L_y , R_x , and R_y across the domain wall are shown. To minimize the scanning noise, the results of unit cells with the same distances (the same unit cell position) to the domain wall are averaged. Figure 2(c) shows the line profiles of L_x and L_y , which stay nearly constant in both two domains and their domain walls. Figure 2(d) shows the line profiles of R_x and R_y . On the one hand, R_x is relatively stable inside every domain but has a small difference

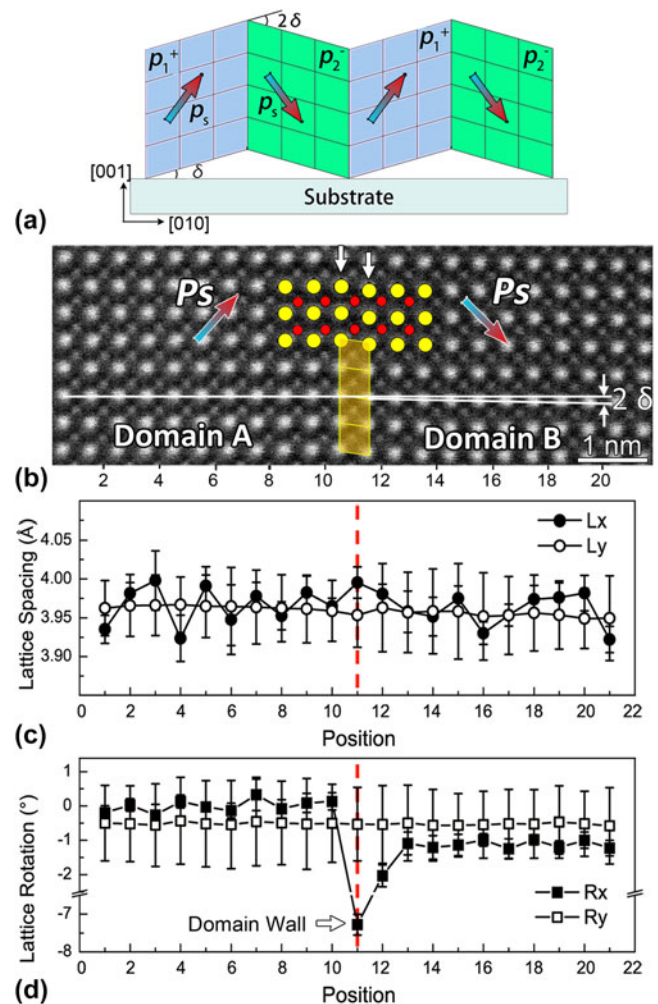


FIG. 2. (a) A schematic of relaxed 109° domains. δ is the mismatch angle between the domain and substrate, and 2δ is the mismatch angle of nearby domains. (b) An atomic resolved HAADF-STEM image of a 109° domain pattern far away from the film/substrate interface (BiFeO₃/GdScO₃) along [100]_P the zone axis. The scale bar is 1 nm. The mismatch angle 2δ between domain A and B is traced. (c-d) Line profiles of L_x , L_y , R_x , and R_y across the domain wall in (b).

~1° between domain A and domain B. This difference precisely represents the mismatch angle 2δ . It is also noticeable that at the domain wall (position 11), R_x drops as large as about 7° (the horizontal lattice rotation of domain A is normalized as zero) which features the domain wall lattice shear distortion. On the other hand, R_y is nearly unchanged in both two domains and the domain walls. It is worthwhile to mention that these characters of lattice distortions at the domain wall can serve as a fingerprint to identify the location of the 109° domain wall. Based on the above analysis, the lattice distortion feature of unstrained 109° domains can be represented in terms of the rhombohedral distortion 2δ and domain wall distortion R_x .

C. Structural features of 109° domains near interface

To maintain an epitaxial relationship, local distortions can be imposed onto a film to match the substrate constraint.^{17,18} Such a kind of boundary condition could play an important role in the properties of thin films especially for a ferroelectric thin film due to the coupling of polarization with the lattice distortion. For the BiFeO₃/GdScO₃ thin film system, although it provides relatively small lateral lattice mismatch, the pinning effect of the film/substrate near the interface would still exist. To clarify such an effect of substrate constraints, we first focus on element intermixing of the interface for the BiFeO₃/GdScO₃ thin film. Figure 3(a) is an atomic-resolved HAADF-STEM image of the BiFeO₃/GdScO₃ thin film recorded along the [100]_P zone axis of BiFeO₃. Electron energy loss spectroscopic (EELS) line scan analysis is performed in the atomic plane marked by the arrow. The corresponding element distributions are revealed, as shown in Fig. 3(b). As the M_{4,5} edges of Bi are out of the acquisition range of the EELS signal in the present study, we use edges of Fe, Pr, and Sc. In Fig. 3(b), intermixing of Fe and Sc indicated by the arrow is resolved, which is within one unit cell.

Figure 4(a) is an atomic resolved HAADF-STEM image of a 109° domain near the BiFeO₃/GdScO₃ interface. The lattice structural features, mismatch angle 2δ, and domain wall lattice rotation R_x of the 109° domain reveal noticeable changes near the interface, comparing with the unstrained one in Fig. 2(b). For the mismatch angle 2δ, it gradually reduces from 1.0° to 0.2° when approaching the interface. For the domain wall shear distortion R_x, a similar trend is illustrated by yellow frames where the shear feature almost disappears near the interface. Quantitative representations of the evolution of 2δ and R_x are shown in Figs. 4(b) and 4(c). In Fig. 4(b),

the mismatch angle 2δ gets to a value of approximately 1° far away from the interface which is similar to the value revealed in Fig. 2(d). This angle begins to reduce at position 16 and finally diminishes to nearly zero at the interface. The reduction of 2δ implies a transition layer of about 16 unit cells in thickness near the interface as depicted by the shadow area in Fig. 4(b). For the domain wall shear distortion in Fig. 4(c), R_x obtains a value of -5° to -7° far away from the interface and gradually reduces to nearly zero from position 27 to position 30. Comparing with the unstrained 109° domain, the suppression of 2δ and R_x near the interface reflects the strong pinning effect of the substrate constraint on the structural features of BiFeO₃.

D. Asymmetrical lattice distortions of 109° domains

The lattice rotation of the domain wall, in fact, connects to a relative shift of the position of nearby domains, for example, the shift of domain B relative to domain A in Fig. 2(b). For the unstrained 109° domain, the shift can be as large as 0.5 Å.³⁴ For the 109° domain near the interface in Fig. 4(a) where the lattice rotation of the domain wall is suppressed when approaching the interface, the corresponding shift of the nearby domains (domain C and domain D) must be compromised, as shown in Fig. 5(a). As a result, the asymmetry distortion of the lattice spacing L_y would emerge. It is expected that the out-of-plane lattice spacing L_y in domain D decreases, while L_y in domain C increases. Such a kind of a situation is convinced in Fig. 5(b), the line profiles of L_y corresponding to domain C and domain D in Fig. 4(a). The L_y far away from the interface maintains a similar value with the unstrained one [Fig. 2(c)]. However, when approaching to the point about 5 unit cells away from the

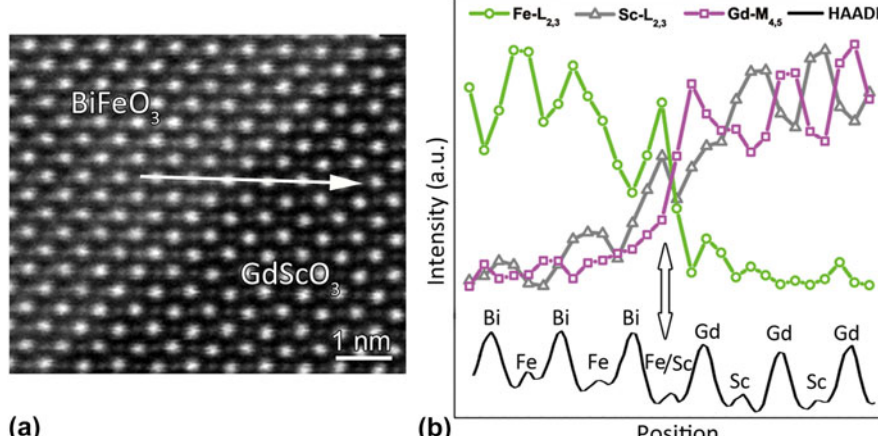


FIG. 3. (a) An atomic-resolved HAADF-STEM image of the BiFeO₃/GdScO₃ interface along [100]_P. EELS line analysis is performed in the atomic plane marked by the arrow. (b) A chemical line profile across the BiFeO₃/GdScO₃ interface. The vertical arrow denotes the position with element intermixing.

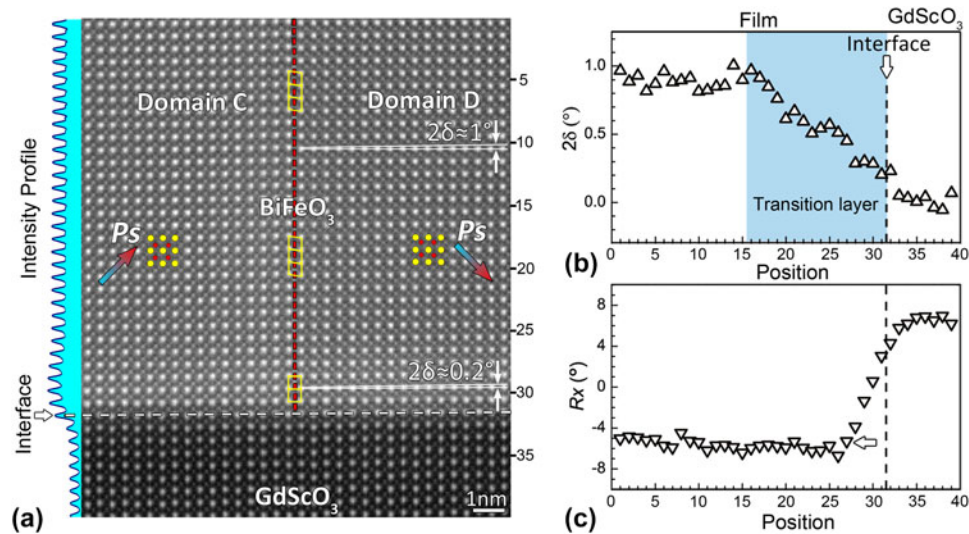


FIG. 4. (a) An atomic-resolved HAADF-STEM image of a 109° domain near the BiFeO₃/GdScO₃ interface along [100]_P. The scale bar is 1 nm. Polarization projection P_s is indicated by the colored arrow base on the Fe sublattice displacement illustrated by the superposed structural model. The location of the domain wall is marked with a vertical dotted line. The left inset is the intensity profile of Fig. 4(a) used to determine the location of the film/substrate interface (white dotted line). Note that the mismatch angle 2δ and domain wall shear distortion R_x vary with the distance from the interface. (b–c) Variation of 2δ and R_x across the BiFeO₃/GdScO₃ interface. Note that 2δ deviates from the bulk value and forms a transition layer near the interface.

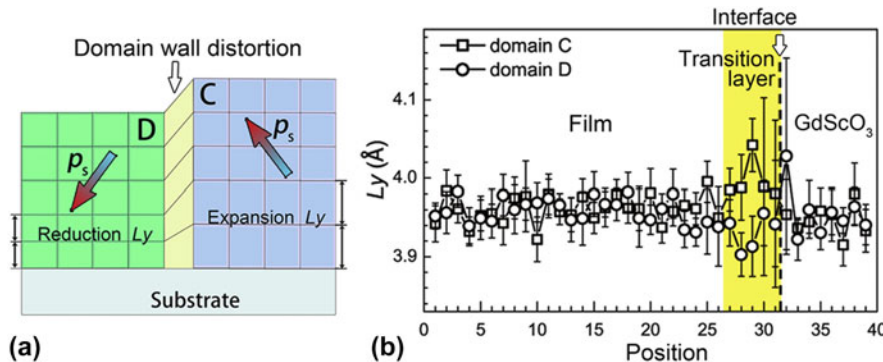


FIG. 5. (a) A schematic of the 109° domain wall distortion near the interface. (b) The line profile of L_y of Fig. 4(a). Note the abnormal expansion/reduction of L_y near the interface.

interface, L_y increases to ~ 4.1 Å in domain C and decreases to ~ 3.9 Å in domain D. The abnormal expansion/reduction of L_y then generates a transition layer of about 2 nm thick (four unit cells). This transition layer, with its thickness much thinner than that of transition layers for 2δ , is a typical feature of the suppression of the relative shifts in adjacent domains (the domain wall shear distortion) due to the substrate constraints.

E. Structural features of 109° domains with large strain state

For the BiFeO₃/GdScO₃ system, the lateral lattice mismatch is rather small, thus the substrate constraints are mainly imposed from the out-of-plane direction. For heterointerfaces with large lateral lattice misfit where in-

plane constraints must be taken into account, whether the above transition layers would still exist is needed to be further explored. The BiFeO₃/PrScO₃ system can provide a lateral mismatch as large as 1.5%. Before going to analyze substrate constraints under such condition, it is worthwhile to check whether the film still maintains the structural features of rhombohedral BiFeO₃ since Zhu et al. reported that an orthogonal phase can be stabilized under large tensile strain by carefully controlling the boundary condition.¹³ For our thin film with about 50 nm in thickness, an apparent 109° stripe domain pattern can be observed,²⁵ which is a character of a rhombohedral-like structure. Similar domain patterns were also observed by Chen et al.³² Furthermore, the Fe sublattice displacements show out-of-plane components, as shown in Fig. 7(a), demonstrating that the BiFeO₃ has

an out-of-plane polarization component which reveals the characteristics of rhombohedral-like BiFeO₃ rather than orthogonal one.^{13,32}

The interfacial element intermixing of the BiFeO₃/PrScO₃ thin film is determined using the EELS line profile which is obtained from the atomic plane marked by the arrow in Fig. 6(a). The element distribution information is shown in Fig. 6(b) where the vertical arrow marks the position of element intermixing. Obvious intermixing of Sc and Fe are resolved, which is also within one unit cell. Figure 7(a) is an atomic resolved HAADF-STEM image of the BiFeO₃/PrScO₃ thin film. The mismatch angle 2δ and domain wall shear distortion R_x across the interface are then quantitatively analyzed. The variation of 2δ versus the unit cell position is shown in Fig. 7(b). 2δ is about 0.8–0.9° far away from the

interface, and gradually reduces to nearly zero at the interface, similar to the tendency of the BiFeO₃/GdScO₃ system. A transition layer of about 6 nm (15 unit cells) is revealed. For the domain wall shear distortion R_x in Fig. 7(c), the average value of R_x away from the interface is around -3° to -4° and also shows a relative reduction near the interface. For lattice spacing L_y in Fig. 7(d), it has an asymmetry distribution in about 2 unit cells near the interface where L_y obtains a local expansion in domain E and a local reduction in domain F. Again, an interfacial layer with abnormal L_y is also introduced. Although the BiFeO₃/PrScO₃ system has a large lateral misfit strain, the rhombohedral-like structural feature is preserved and interfacial transition layers are still kept. For the interfacial layer with abnormal out-of-plane lattice spacing, it is a typical feature of the suppression of the 109° domain

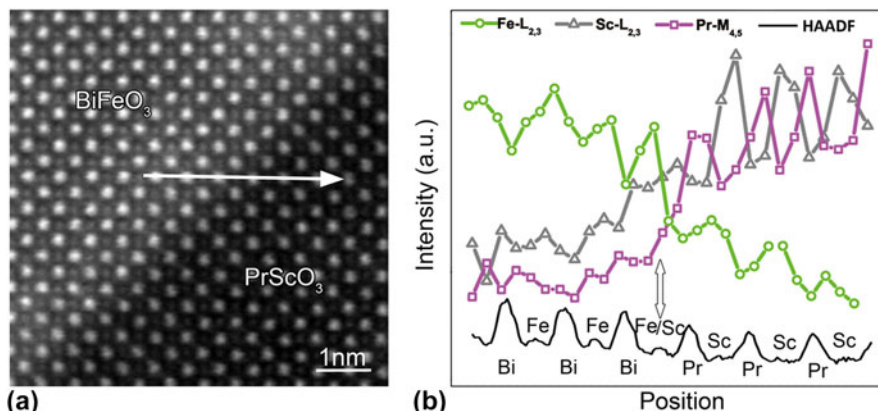


FIG. 6. (a) An atomic-resolved HAADF-STEM image of the BiFeO₃/PrScO₃ interface along [100]_P. EELS line analysis is carried out in the atomic plane marked by the arrow. (b) A chemical line profile across the BiFeO₃/PrScO₃ interface. The vertical arrow denotes the position with element intermixing.

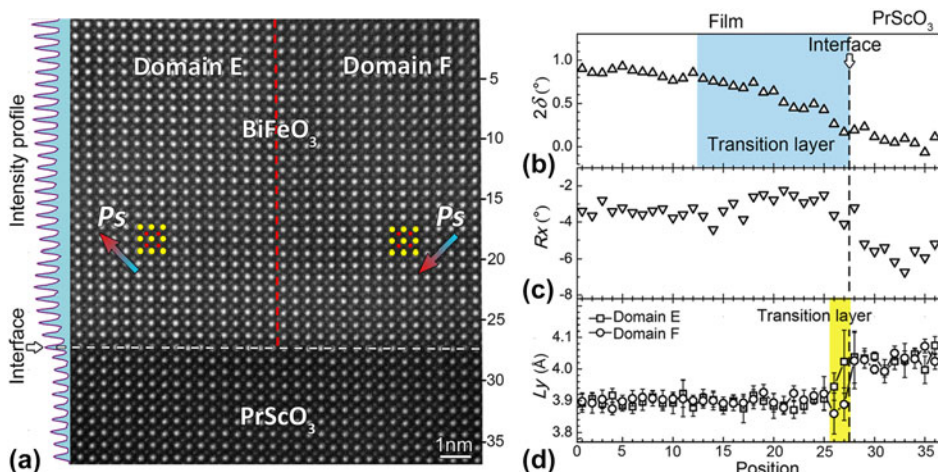


FIG. 7. (a) An atomic-resolved HAADF-STEM image of a 109° domain near the BiFeO₃/PrScO₃ interface. The scale bar is 1 nm. Polarization projections P_s of domain E and F are indicated by arrows base on the Fe sublattice displacement illustrated by the superposed structural model. The location of domain wall is marked with a vertical dotted line. The left inset is the intensity profile of Fig. 7(a) used to determine the location of the film/substrate interface (horizontal dotted line). (b-d) Variations of the domain mismatch angle 2δ , domain wall shear feature R_x , and vertical lattice spacing L_y across the BiFeO₃/PrScO₃ interface.

wall distortion, and its existence then is expected to be a universal behavior in such 109° patterned rhombohedral-like BiFeO₃ thin films resulting from substrate constraints.

IV. DISCUSSIONS

It is worthwhile to note that the rhombohedral distortion (2δ) and domain wall shear distortion (R_x) are all suppressed near interfaces in thin films with different lateral misfit strains (BiFeO₃/GdScO₃ and BiFeO₃/PrScO₃). The rhombohedral distortion, which features the interlattice angle of the rhombohedral unit cell ($90 - \delta$), shows an inhomogeneous distribution with a suppression layer of several nanometers (about 6 nm) thick starting from the interface to the film. Beyond this thickness, the rhombohedral distortion keeps the same value as in the bulk form (about 1° for BiFeO₃). For the shear feature R_x of 109° domain walls, although it reduces at several unit cells thick area near the film/substrate interface, the relatively small suppression area implies that the interface pinning effect on R_x decreases rapidly away from the interface. In addition, the tensile strain would reduce the total magnitude of R_x (-5° to -7° for BiFeO₃/GdScO₃, -3° to -4° for BiFeO₃/PrScO₃). It is believed that the domain wall distortion would be further suppressed under large lateral tensile constraints, and the thickness of the interfacial layer (abnormal L_y) would further reduce (~ 5 unit cells for BiFeO₃/GdScO₃, ~ 2 unit cells for BiFeO₃/PrScO₃). Thus by choosing substrates with suitable lateral constraints, the manipulation on the thickness of the abnormal L_y interfacial layer would be highly possible.

The local structural distortions near/at interfaces, i.e., the abnormal layer, are of importance for novel properties dominated by the interface, which are sensitive to the interplay of different order parameters at the interface. For BiFeO₃ thin films, it has been demonstrated that many aspects connect to the abnormal L_y , such as octahedral rotation,³⁶ concentration of oxygen vacancies,³⁷ and abnormal ferroelectric dipoles³⁸ near/at interfaces. Borisevich et al. reported that the accommodation of octahedral rotation near BiFeO₃/La_{0.7}Sr_{0.3}MnO₃ interface can introduce an interface phase with novel magnetic properties and abnormal increase of out-of-plane lattice spacing L_y .³⁶ Kim et al. explained that abnormal lattice expansion near the BiFeO₃/La_{0.7}Sr_{0.3}MnO₃ interface comes from the vacancy-induced local stabilization of the high c/a phase.³⁷ Although these structural features are quite complicated for the perovskite oxide system, it is of interest to note that the expanded or reduced out-of-plane lattice parameters near the interface are connected with the domain wall distortion in the present study. In other words, it is the nearby domain relationship that promises certain domain wall distortions and triggers the interfacial

structural distortions. Thus, it is expected that by domain engineering, the novel structural feature can be manipulated at the local area near/at heterointerfaces for ferroic thin films, promising another approach seeking for interface dominated properties.

V. CONCLUSIONS

In this paper, we demonstrate at the atomic level the structural distortions in two kinds of 109° domain patterned BiFeO₃ thin films with different tensile strain states. Structural features including the mismatch angle (2δ) and domain wall shear distortion (R_x) are quantitatively analyzed which are found to be suppressed near the interfaces due to the substrate constraints. An additional interfacial layer with expanded and reduced out-of-plane lattice spacing is resolved. These interfacial structural distortions are a typical character of the interplay of intrinsic spontaneous structural distortions with external substrate constraints, which implies a potential mediation of interfacial structures by domain engineering in ferroic thin films.

ACKNOWLEDGMENTS

This work is supported by the National Natural Science Foundation of China (Nos. 51231007, 51571197, 51501194, 51671194, and 51521091), National Basic Research Program of China (2014CB921002), and the Key Research Program of Frontier Sciences, CAS (QYZDJ-SSW-JSC010). Y.L.T. acknowledges the IMR SYNL-T.S. Kê Research Fellowship and the Youth Innovation Promotion Association CAS (No. 2016177).

REFERENCES

1. J.F. Scott: Applications of modern ferroelectrics. *Science* **315**, 954 (2007).
2. N.A. Spaldin and M. Fiebig: The renaissance of magnetoelectric multiferroics. *Science* **309**, 391 (2005).
3. L.W. Martin and R. Ramesh: Multiferroic and magnetoelectric heterostructures. *Acta Mater.* **60**, 2449 (2012).
4. D.G. Schlom, L-Q. Chen, C-B. Eom, K.M. Rabe, S.K. Streiffer, and J-M. Triscone: Strain tuning of ferroelectric thin films. *Annu. Rev. Mater. Res.* **37**, 589 (2007).
5. D.G. Schlom, L-Q. Chen, C.J. Fennie, V. Gopalan, D.A. Muller, X. Pan, R. Ramesh, and R. Uecker: Elastic strain engineering of ferroic oxides. *MRS Bull.* **39**, 118 (2014).
6. J.H. Lee, L. Fang, E. Vlahos, X. Ke, Y.W. Jung, L.F. Kourkoutis, J.W. Kim, P.J. Ryan, T. Heeg, M. Roeckerath, V. Goian, M. Bernhagen, R. Uecker, P.C. Hammel, K.M. Rabe, S. Kamba, J. Schubert, J.W. Freeland, D.A. Muller, C.J. Fennie, P. Schiffer, V. Gopalan, E. Johnston-Halperin, and D.G. Schlom: A strong ferroelectric ferromagnet created by means of spin-lattice coupling. *Nature* **466**, 954 (2010).
7. J.H. Haeni, P. Irvin, W. Chang, R. Uecker, P. Reiche, Y.L. Li, S. Choudhury, W. Tian, M.E. Hawley, B. Craig, A.K. Tagantsev, X.Q. Pan, S.K. Streiffer, L.Q. Chen, S.W. Kirchoefer, J. Levy, and D.G. Schlom: Room-temperature ferroelectricity in strained SrTiO₃. *Nature* **430**, 758 (2004).

8. K.J. Choi, M. Biegalski, Y.L. Li, A. Sharan, J. Schubert, R. Uecker, P. Reiche, Y.B. Chen, X.Q. Pan, V. Gopalan, L-Q. Chen, D.G. Schlom, and C.B. Eom: Enhancement of ferroelectricity in strained BaTiO₃ thin films. *Science* **306**, 1005 (2004).
9. G. Catalan, A. Lubk, A.H.G. Vlooswijk, E. Snoeck, C. Magen, A. Janssens, G. Rispens, G. Rijnders, D.H.A. Blank, and B. Noheda: Flexoelectric rotation of polarization in ferroelectric thin films. *Nat. Mater.* **10**, 963 (2011).
10. Y.L. Tang, Y.L. Zhu, X.L. Ma, A.Y. Borisevich, A.N. Morozovska, E.A. Eliseev, W.Y. Wang, Y.J. Wang, Y.B. Xu, Z.D. Zhang, and S.J. Pennycook: Observation of a periodic array of flux-closure quadrants in strained ferroelectric PbTiO₃ films. *Science* **348**, 547 (2015).
11. I.C. Infante, S. Lisenkov, B. Dupé, M. Bibes, S. Fusil, E. Jacquet, G. Geneste, S. Petit, A. Courtial, J. Juraszek, L. Bellaiche, A. Barthélémy, and B. Dkhil: Bridging multiferroic phase transitions by epitaxial strain in BiFeO₃. *Phys. Rev. Lett.* **105**, 057601 (2010).
12. R.J. Zeches, M.D. Rossell, J.X. Zhang, A.J. Hatt, Q. He, C.H. Yang, A. Kumar, C.H. Wang, A. Melville, C. Adamo, G. Sheng, Y.H. Chu, J.F. Ihlefeld, R. Erni, C. Ederer, V. Gopalan, L.Q. Chen, D.G. Schlom, N.A. Spaldin, L.W. Martin, and R. Ramesh: A strain-driven morphotropic phase boundary in BiFeO₃. *Science* **326**, 977 (2009).
13. J.C. Yang, Q. He, S.J. Suresha, C.Y. Kuo, C.Y. Peng, R.C. Haislmaier, M.A. Motyka, G. Sheng, C. Adamo, H.J. Lin, Z. Hu, L. Chang, L.H. Tjeng, E. Arenholz, N.J. Podraza, M. Bernhagen, R. Uecker, D.G. Schlom, V. Gopalan, L.Q. Chen, C.T. Chen, R. Ramesh, and Y.H. Chu: Orthorhombic BiFeO₃. *Phys. Rev. Lett.* **109**, 247606 (2012).
14. Y.H. Chu, M.P. Cruz, C.H. Yang, L.W. Martin, P.L. Yang, J.X. Zhang, K. Lee, P. Yu, L.Q. Chen, and R. Ramesh: Domain control in multiferroic BiFeO₃ through substrate vicinality. *Adv. Mater.* **19**, 2662 (2007).
15. Y.H. Chu, Q. Zhan, L.W. Martin, M.P. Cruz, P.L. Yang, G.W. Pabst, F. Zavaliche, S.Y. Yang, J.X. Zhang, L.Q. Chen, D.G. Schlom, I.N. Lin, T.B. Wu, and R. Ramesh: Nanoscale domain control in multiferroic BiFeO₃ thin films. *Adv. Mater.* **18**, 2307 (2006).
16. J. Seidel: Domain walls as nanoscale functional elements. *J. Phys. Chem. Lett.* **3**, 2905 (2012).
17. S.K. Streiffer, C.B. Parker, A.E. Romanov, M.J. Lefevre, L. Zhao, J.S. Speck, W. Pompe, C.M. Foster, and G.R. Bai: Domain patterns in epitaxial rhombohedral ferroelectric films. I. Geometry and experiments. *J. Appl. Phys.* **83**, 2742 (1998).
18. A.E. Romanov, M.J. Lefevre, J.S. Speck, W. Pompe, S.K. Streiffer, and C.M. Foster: Domain pattern formation in epitaxial rhombohedral ferroelectric films. II. Interfacial defects and energetics. *J. Appl. Phys.* **83**, 2754 (1998).
19. C.W. Huang, Z.H. Chen, and L. Chen: Thickness-dependent evolutions of domain configuration and size in ferroelectric and ferroelectric-ferroelastic films. *J. Appl. Phys.* **113**, 094101 (2013).
20. C.W. Huang, L. Chen, J. Wang, Q. He, S.Y. Yang, Y.H. Chu, and R. Ramesh: Phenomenological analysis of domain width in rhombohedral BiFeO₃ films. *Phys. Rev. B* **80**, 140101 (2009).
21. J.E. Giencke, C.M. Folkman, S.H. Baek, and C.B. Eom: Tailoring the domain structure of epitaxial BiFeO₃ thin films. *Curr. Opin. Solid State Mater. Sci.* **18**, 39 (2014).
22. L. Li, P. Gao, C.T. Nelson, J.R. Jokisaari, Y. Zhang, S-J. Kim, A. Melville, C. Adamo, D.G. Schlom, and X. Pan: Atomic scale structure changes induced by charged domain walls in ferroelectric materials. *Nano Lett.* **13**, 5218 (2013).
23. C.T. Nelson, B. Winchester, Y. Zhang, S-J. Kim, A. Melville, C. Adamo, C.M. Folkman, S-H. Baek, C-B. Eom, D.G. Schlom, L-Q. Chen, and X. Pan: Spontaneous vortex nanodomain arrays at ferroelectric heterointerfaces. *Nano Lett.* **11**, 828 (2011).
24. W-Y. Wang, Y-L. Tang, Y-L. Zhu, Y-B. Xu, Y. Liu, Y-J. Wang, S. Jagadeesh, and X-L. Ma: Atomic level 1D structural modulations at the negatively charged domain walls in BiFeO₃ films. *Adv. Mater. Interfaces* **2**, 1500024 (2015).
25. W.Y. Wang, Y.L. Zhu, Y.L. Tang, Y.B. Xu, Y. Liu, S. Li, S.R. Zhang, Y.J. Wang, and X.L. Ma: Large scale arrays of four-state vortex domains in BiFeO₃ thin film. *Appl. Phys. Lett.* **109**, 202904 (2016).
26. R.P. Liferovich and R.H. Mitchell: A structural study of ternary lanthanide orthoscorpionate perovskites. *J. Solid State Chem.* **177**, 2188 (2004).
27. S.M. Anthony and S. Granick: Image analysis with rapid and accurate two-dimensional Gaussian fitting. *Langmuir* **25**, 8152 (2009).
28. Y.H. Chu, Q. He, C.H. Yang, P. Yu, L.W. Martin, P. Shafer, and R. Ramesh: Nanoscale control of domain architectures in BiFeO₃ thin films. *Nano Lett.* **9**, 1726 (2009).
29. J. Seidel, L.W. Martin, Q. He, Q. Zhan, Y.H. Chu, A. Rother, M.E. Hawkridge, P. Maksymovych, P. Yu, M. Gajek, N. Balke, S.V. Kalinin, S. Gemming, F. Wang, G. Catalan, J.F. Scott, N.A. Spaldin, J. Orenstein, and R. Ramesh: Conduction at domain walls in oxide multiferroics. *Nat. Mater.* **8**, 229 (2009).
30. Q. He, C.H. Yeh, J.C. Yang, G. Singh-Bhalla, C.W. Liang, P.W. Chiu, G. Catalan, L.W. Martin, Y.H. Chu, J.F. Scott, and R. Ramesh: Magnetotransport at domain walls in BiFeO₃. *Phys. Rev. Lett.* **108**, 067203 (2012).
31. Z.H. Chen, A.R. Damodaran, R. Xu, S. Lee, and L.W. Martin: Effect of "symmetry mismatch" on the domain structure of rhombohedral BiFeO₃ thin films. *Appl. Phys. Lett.* **104**, 182908 (2014).
32. Z. Chen, Y. Qi, L. You, P. Yang, C.W. Huang, J. Wang, T. Sritharan, and L. Chen: Large tensile-strain-induced M_B phase in BiFeO₃ epitaxial thin films on a PrScO₃. *Phys. Rev. B* **88**, 054114 (2013).
33. Y.J. Qi, Z.H. Chen, C.W. Huang, L.H. Wang, X.D. Han, J.L. Wang, P. Yang, T. Sritharan, and L. Chen: Coexistence of ferroelectric vortex domains and charged domain walls in epitaxial BiFeO₃ film on (110)_O GdScO₃ substrate. *J. Appl. Phys.* **111**, 104117 (2012).
34. A. Lubk, M.D. Rossell, J. Seidel, Q. He, S.Y. Yang, Y.H. Chu, R. Ramesh, M.J. Hÿtch, and E. Snoeck: Evidence of sharp and diffuse domain walls in BiFeO₃ by means of unit-cell-wise strain and polarization maps obtained with high resolution scanning transmission electron microscopy. *Phys. Rev. Lett.* **109**, 047601 (2012).
35. Y. Wang, C. Nelson, A. Melville, B. Winchester, S. Shang, Z-K. Liu, D.G. Schlom, X. Pan, and L.Q. Chen: BiFeO₃ domain wall energies and structures: A combined experimental and density functional theory + U study. *Phys. Rev. Lett.* **110**, 267601 (2013).
36. A.Y. Borisevich, H.J. Chang, M. Huijben, M.P. Oxley, S. Okamoto, M.K. Niranjan, J.D. Burton, E.Y. Tsymbal, Y.H. Chu, P. Yu, R. Ramesh, S.V. Kalinin, and S.J. Pennycook: Suppression of octahedral tilts and associated changes in electronic properties at epitaxial oxide heterostructure interfaces. *Phys. Rev. Lett.* **105**, 087204 (2010).
37. Y.M. Kim, A. Morozovska, E. Eliseev, M.P. Oxley, R. Mishra, S.M. Selbach, T. Grande, S.T. Pantelides, S.V. Kalinin, and A.Y. Borisevich: Direct observation of ferroelectric field effect and vacancy-controlled screening at the BiFeO₃/La_xSr_{1-x}MnO₃ interface. *Nat. Mater.* **13**, 1019 (2014).
38. R. Huang, H-C. Ding, W-I. Liang, Y-C. Gao, X-D. Tang, Q. He, C-G. Duan, Z. Zhu, J. Chu, C.A.J. Fisher, T. Hirayama, Y. Ikuhara, and Y-H. Chu: Atomic-scale visualization of polarization pinning and relaxation at coherent BiFeO₃/LaAlO₃ interfaces. *Adv. Funct. Mater.* **24**, 793 (2014).